Supporting Information for "Stochastic interpretation of the advection diffusion equation and its relevance to bed load transport"

C. Ancey[1], P. Bohórquez[2], and J. Heyman[1]

Contents of this file

1. Lagrangian point of view in the advection diffusion equation: how can simple random walk models be used to derive the advection diffusion equation (1) in the paper (without the source term)?

2. Approximation of the forward Kolmogorov equation: how can the forward Kolmogorov equation (11) in the paper be solved approximately using a Taylor expansion?

C. Ancey, School of Architecture, Civil and Environmental Engineering, École Polytechnique Fédérale de Lausanne, 1015 Lausanne, Switzerland (christophe.ancey@epfl.ch)

[1]School of Architecture, Civil and Environmental Engineering, École Polytechnique Fédérale de Lausanne, 1015 Lausanne, Switzerland

[2]Ingeniería Mecánica y Minera, Universidad de Jaén, 23071 Jaén, Spain

3. Poisson representation and exact Langevin equations: how can the forward Kolmogorov equation (11) in the paper be solved exactly using an exact technique called the Poisson representation?

4. Analysis of the Langevin representation of b: how are the statistical properties of b [equation (21) in the paper] derived?

5. Euler scheme for solving the Langevin equations for a_i: how to solve the Langevin equations [equation (15) in the paper] numerically?

6. Iterative calculation of the spatial cross correlations: additional proof for section 3.3.

7. Iterative calculation of the autocorrelation time: how is the approximate autocorrelation function [equation (33) in the paper] obtained?

8. Stability condition of a central explicit scheme for Langevin equation: additional proof for the stability of the central difference scheme.

9. Variance of diffusive processes: how is the cell variance [equation (37) in the paper] obtained?

10. Simulation of advection and diffusion: additional results showing the effect of the emigration ν in advection-diffusion processes.

11. Analytic solution to the pure advection problem considered in section 3 in the paper.

12. Expressing $\langle \boldsymbol{a} \rangle$ as a convolution sum (section 3.3 in the paper).

1. Lagrangian point of view in the advection diffusion equation

Let us consider a particle that moves incrementally along an axis x (see Figure 1). This particle can jump to the right (with constant probability p) or to the left (with probability

q) at each time step $t = k\tau$ with $k = 0, 1, 2 \ldots$ [*Zauderer*, 1983]. The jump length takes the fixed value δ. The time step τ is also fixed. There is a constant probability r that the particle stays at the same place at each time step. The laws of probability imposes that $p+q+r = 1$. We denote by Δx_k the displacement made by the particle at time step $t = k\tau$.

Without any loss of generality, we can express the transition probabilities for each time step in terms of a constant δ_0 (to be determined) and the parameters r and δ.

$$P(x \to x+\delta, t = k\tau) \;=\; p = \frac{1}{2}\left(1 - r + \frac{\delta}{\delta_0}\right) \tag{1}$$

$$P(x \to x-\delta, t = k\tau) \;=\; q = \frac{1}{2}\left(1 - r - \frac{\delta}{\delta_0}\right) \tag{2}$$

$$P(x \to x, t = k\tau) \;=\; r. \tag{3}$$

The distance traveled by the particle after k time steps is $X_k = \sum_{i=0}^{k} \Delta x_k$. As $\langle \Delta x_k \rangle = p\delta - q\delta + r \times 0 = (p-q)\delta$, it is straightforward to calculate its mean value

$$\langle X_k \rangle = \sum_{i=0}^{k} \langle \Delta x_i \rangle = k(p-q)\delta = \frac{t}{\tau}\frac{\delta^2}{\delta_0} \tag{4}$$

As the jumps are independent random events, the variance of the total displacement equals the sum of the variances of the random events

$$\mathrm{var} X_k \;=\; \sum_{i=0}^{k} \langle \Delta x_i^2 \rangle - \langle \Delta x_i \rangle^2 \tag{5}$$

$$\;=\; \sum_{i=0}^{k} \left(p\delta^2 + q\delta^2 - \langle \Delta x_i \rangle^2 \right) = \left(1 - r - \frac{\delta^2}{\delta_0^2}\right) \delta^2 \frac{t}{\tau} \tag{6}$$

We now take the continuum limit $\tau \to 0$ and $\delta \to 0$ and try to see whether a macroscopic behavior emerges from this limit. From the mean displacement equation (4), a nonzero finite limit of $\langle X_k \rangle$ is achieved if we set

$$\lim_{\tau \to 0, \delta \to 0} \frac{\delta^2}{\tau \delta_0} = u \tag{7}$$

where u is a constant value interpreted as the drift velocity. This limit imposes the scaling $\delta^2 \propto \tau$. From the variance equation (5), we deduce that a nonzero finite limit of $\mathrm{var}X_k$ is obtained by setting

$$\lim_{\tau\to 0,\delta\to 0} \left(1 - r - \frac{\delta^2}{\delta_0^2}\right) \frac{\delta^2}{\tau} = (1-r)\frac{\delta^2}{\tau} = 2D \tag{8}$$

where D is a constant value interpreted as the diffusivity. Note that equation (8) is fully consistent with the scaling $\delta^2 \propto \tau$. In summary, we have found that in the continuum limit $\tau \to 0$ and $\delta \to 0$, the random walk can be characterized by the mean displacement $\langle X \rangle$ and the fluctuations (encoded through $\mathrm{var}X$)

$$\langle X \rangle(t) = ut \text{ and } \mathrm{var}X(t) = 2Dt \tag{9}$$

The macroscopic parameters u and D are related to the microscopic parameters r and δ_0

$$\frac{\delta_0}{1-r} = 2\frac{D}{u} \tag{10}$$

So, the knowledge of the macroscopic behavior of the particle leads to partial information on the local behavior: the parameters r and δ_0 are linked through equation (10), but they are not uniquely determined.

Let us now derive the advection diffusion equation. To that end, let us consider the probability of finding the particle at position x at time $t + \tau$. At the previous time increment, the particle was at the same place (with probability r), at $x - \delta$ (and so jumped to the right with probability p), or at $x + \delta$ (and so jumped to the left with probability q)

$$P(x, t+\tau) = rP(x,t) + pP(x-\delta, t) + qP(x+\delta, t) \tag{11}$$

A Taylor expansion (order 2 in space, order 1 in time, higher orders leads to vanishingly small values) leads to

$$P(x,t) + \tau \frac{\partial}{\partial t} P(x,t) = rP(x,t) + p\left(P(x,t) - \delta \frac{\partial}{\partial x} P(x,t) + \frac{\delta^2}{2} \frac{\partial^2}{\partial x^2} P(x,t) \right) + q\left(P(x,t) + \delta \frac{\partial}{\partial x} P(x,t) + \frac{\delta^2}{2} \frac{\partial^2}{\partial x^2} P(x,t) \right) \quad (12)$$

Collecting the terms, we get

$$\frac{\partial}{\partial t} P(x,t) = -\frac{\delta}{\tau}(p-q) \frac{\partial}{\partial x} P(x,t) + \frac{\delta^2}{2\tau}(p+q) \frac{\partial^2}{\partial x^2} P(x,t) \quad (13)$$

In the continuum limit, making use of equation (7) and equation (8) leads to the desired result

$$\frac{\partial}{\partial t} P(x,t) = -u \frac{\partial}{\partial x} P(x,t) + D \frac{\partial^2}{\partial x^2} P(x,t) \quad (14)$$

The derivation above holds for $D > 0$. For $D = 0$ (pure advection), the expression of the transition probabilities must be changed into

$$P(x \to x + \delta, t = k\tau) \; = \; p = \frac{1}{2}(1 - r_1 + r_2) \quad (15)$$

$$P(x \to x - \delta, t = k\tau) \; = \; q = \frac{1}{2}(1 - r_1 - r_2) \quad (16)$$

$$P(x \to x, t = k\tau) \; = \; r_1. \quad (17)$$

where r_1 and r_2 are constant parameters. The mean displacement $\langle X_k \rangle = k(p-q)\delta$ admits a nonzero finite value if we set

$$\lim_{\tau \to 0, \delta \to 0} r_2 \frac{\delta}{\tau} = u \quad (18)$$

implying the scaling $\delta \propto \tau$. The variance become vanishing small

$$\lim_{\tau \to 0, \delta \to 0} \mathrm{var} X_k = \lim_{\tau \to 0, \delta \to 0} \frac{\delta^2}{\tau}(1 - r_1 + r_2)t = 0 \quad (19)$$

In that case, the governing equation at the macroscopic scale is the advection equation

$$\frac{\partial}{\partial t} P(x,t) = -u \frac{\partial}{\partial x} P(x,t) \quad (20)$$

2. Approximation of the forward Kolmogorov equation

An approximation of the forward Kolmogorov equation (11) in the paper

$$\begin{aligned}\frac{\partial P}{\partial t}(\boldsymbol{n};t) \;=\; & \sum_{i=1}^{M}(n_i+1)(P(\boldsymbol{n}+\boldsymbol{r}_{i+1}^{i},t)\nu_i + P(\boldsymbol{n}+\boldsymbol{r}_i^{+},t)\sigma_i) \\ & +P(\boldsymbol{n}+\boldsymbol{r}_i^{-},t)(\lambda_i+\mu_i(n_i-1)) \\ & +P(\boldsymbol{n}+\boldsymbol{r}_i^{i-1},t)\nu_{i-1}n_{i-1} \\ & -P(\boldsymbol{n},t)(\nu_{i-1}n_{i-1}+\lambda_i+\mu_i n_{i+1}+\nu_i n_i+\sigma_i n_i)\end{aligned} \tag{21}$$

can be found by transforming the discrete probabilities into continuous probability density functions and using Taylor expansions

$$P(\cdots,n_i+1,\cdots) = P(\cdots,n_i,\cdots) + \frac{\partial P}{\partial N_i} + \frac{1}{2}\frac{\partial^2 P}{\partial N_i^2}, \tag{22}$$

and in doing so, we can approximate the forward Kolmogorov equation by a multidimensional Langevin or Fokker-Planck equation. To that end, we first calculate the mean change of state per unit time

$$\boldsymbol{A} = \frac{1}{\mathrm{d}t}\mathrm{E}(\Delta\boldsymbol{n}) = \frac{1}{\mathrm{d}t}\sum_{k=1}^{3} p^k \Delta\boldsymbol{n} = \begin{pmatrix} \vdots \\ \nu_i n_{i-1} + \lambda_i + (\mu_i - \sigma_i - \nu_{i+1})n_i \\ \vdots \end{pmatrix} \tag{23}$$

We also calculate the covariance matrix

$$\begin{aligned}\boldsymbol{B} \;&=\; \frac{1}{\mathrm{d}t}\mathrm{E}(\Delta\boldsymbol{n}\Delta\boldsymbol{n}^{\dagger}) \\ &=\; \frac{1}{\mathrm{d}t}\sum_{k=1}^{3} p^k \Delta\boldsymbol{n}\Delta\boldsymbol{n}^{\dagger} \\ &=\; \begin{pmatrix} \ddots & \ddots & & \ddots & \ddots & \\ \cdots & 0 & -\nu_i n_{i-1} & \nu_i n_{i-1}+\lambda_i+(\mu_i+\sigma_i+\nu_{i+1})n_i & -\nu_{i+1}n_i & 0 & \cdots \\ & \cdots & \ddots & \ddots & \ddots & \ddots & \end{pmatrix}\end{aligned} \tag{24}$$

Using Taylor expansions of P, it can be shown that the forward Kolmogorov equation (21) can be approximated by the Langevin equation [*Allen*, 2007]

$$\mathrm{d}\boldsymbol{N} = \boldsymbol{A}\mathrm{d}t + \boldsymbol{B}^{1/2}\mathrm{d}\boldsymbol{W} \text{ and } \boldsymbol{N} \geq 0, \tag{25}$$

where $\boldsymbol{W}$ is a vector of length M whose entries are independent Wiener process and $\boldsymbol{B}^{1/2}$ denotes the square root of $\boldsymbol{B}$. The square root of the tridiagonal matrix $\boldsymbol{B}$ may be tractable analytically, but it involves intense calculations for high-dimension problems [*Vandebril et al.*, 2008]. To simplify the calculations, we follow *Gillespie* [2001] and write the covariance matrix $\boldsymbol{B}$ as the product of an $M \times (3M+1)$ matrix $\boldsymbol{C}$

$$\boldsymbol{B} = \boldsymbol{C} \cdot \boldsymbol{C}^{\dagger} \tag{26}$$

with

$$\boldsymbol{C} = \begin{pmatrix} \sqrt{\nu_1 n_0} & \sqrt{\alpha_1} & -\sqrt{\sigma_1 n_1} & -\sqrt{\nu_2 n_1} & 0 & 0 & 0 & 0 \ldots \\ 0 & 0 & 0 & \sqrt{\nu_2 n_1} & \sqrt{\alpha_2} & -\sqrt{\sigma_2 n_2} & -\sqrt{\nu_3 n_2} & 0 \ldots \\ \vdots & & & & & & & \\ 0 & \ldots & 0 & \sqrt{\nu_M n_{M-1}} & \sqrt{\alpha_M} & -\sqrt{\sigma_M n_M} & -\sqrt{\nu_{M+1} n_M} & \end{pmatrix} \tag{27}$$

with $\alpha_i = \lambda_i + \mu_i n_i$ In other words, we can write the entries of $\boldsymbol{C}$ for $1 < i < M$:

- For $j \leq 3(i-1)$, then $C_{ij} = 0$
- There are four nonzero entries: $C_{i,3i-2} = \sqrt{\nu_i n_{i-1}}$, $C_{i,3i-1} = \sqrt{\lambda_i + \mu_i n_i}$, $C_{i,3i} = -\sqrt{\sigma_i n_i}$, and $C_{i,3i+1} = -\sqrt{\nu_{i+1} n_i}$
- For $j > 3i+1$, then $C_{ij} = 0$

Let us now consider that $\boldsymbol{W}$ is a vector of length $3M+1$ whose entries are independent Wiener process, then with no loss of generality, we can transform equation (25) into

$$\mathrm{d}\boldsymbol{N} = \boldsymbol{A}\mathrm{d}t + \boldsymbol{C} \cdot \mathrm{d}\boldsymbol{W} \text{ and } \boldsymbol{N} \geq 0 \tag{28}$$

This system of equations can be solved numerically (see section 5).

3. Poisson representation and exact Langevin equations

Here we show how to solve the forward Kolmogorov equation (21) using the Poisson representation, which is an exact technique in contrast with the approximate technique

seen above. In both cases, we end up with Langevin equations, but not in the same functional space.

3.1. Generating functions

In our last paper [*Ancey and Heyman*, 2014], we followed *Gardiner* [1983] and introduced the Poisson representation, which is an exact technique to transform master equations involving discrete probabilities into Fokker-Planck equations involving continuous probabilities. The technique consists of introducing the generating function and determining the dual operator associated with it.

For one-variable problems, the generating function is

$$G(s,t) = \sum_{n=0}^{\infty} s^n P(n,t) \tag{29}$$

Simple algebraic manipulations allow us to pass from the forward Kolmogorov equation (21) to a partial differential equation for G. For instance, whenever we meet terms like $(n+1)P(n+1,t)$, the corresponding term of the generating function is

$$\sum_{n=0}^{\infty}(n+1)s^n P(n+1,t) = \frac{\partial G}{\partial s} \tag{30}$$

In short, we thus have the following rules

$$\begin{aligned}(n+1)P(n+1,t) &\rightarrow \frac{\partial G}{\partial s}\\ P(n-1,t) &\rightarrow sG\\ nP(n,t) &\rightarrow s\frac{\partial G}{\partial s}\end{aligned}$$

For M-dimension problems, the generating function is

$$G(\boldsymbol{s},t) = \sum_{n_1=0}^{\infty}\sum_{n_2=0}^{\infty}\cdots\sum_{n_M=0}^{\infty}\prod_{i=1}^{M} s_i^{n_i} P(\boldsymbol{n},t). \tag{31}$$

When multiplying the master equation (21) by $s_i^{n_i}$ and summing, the terms like

$$n_i P(\cdots, n_{i-1}, n_i + 1, n_{i+1} - 1, n_{i+2}, \cdots)$$

become $s_{i+1}\partial_{s_i} G$. Similarly, terms like

$$n_i P(\cdots, n_{i-1}, n_i, n_{i+1}, n_{i+2}, \cdots)$$

become $s_i \partial_{s_i} G$. With these rules in mind, we can transform equation (21) into

$$\frac{\partial}{\partial t} G = \sum_{i=1}^{M} \left[\lambda_i (s_i - 1) + \left(\sigma_i + \mu_i s_i^2 + \nu_{i+1} s_{i+1} - (\sigma_i + \mu_i + \nu_i) s_i \right) \frac{\partial}{\partial s_i} G \right] \tag{32}$$

3.2. Poisson representation

The advection equation (32) is quite complicated to analyze and solve for multi-variable systems. Another more instructive form can be derived using the Poisson representation, a sort of Laplace transform [*Gardiner*, 1983]. We expand the state probability as a superposition of Poisson processes of rate $\boldsymbol{a} = (a_i)$

$$P(\boldsymbol{n}, t) = \int_{a_i} \prod_{i=1}^{M} \frac{\mathrm{e}^{-a_i} a_i^{n_i}}{n_i!} f(\boldsymbol{a}, t) \mathrm{d}\alpha_i \tag{33}$$

where $f(\boldsymbol{a}, t)$ is the probability density function of a_i in cell i. The generating function (31) can be written

$$G(\boldsymbol{s}, t) = \int_{a_i} \exp\left(- \sum_{i=1}^{M} a_i (s_i - 1) \right) f(\boldsymbol{a}, t) \mathrm{d}\alpha_i \tag{34}$$

which can be seen as the scalar product (in an appropriate functional space)

$$G(\boldsymbol{s}, t) = \{K, g\}, \text{ where } K = \exp\left(- \sum_{i=1}^{M} a_i (s_i - 1) \right) \tag{35}$$

is the Laplace kernel function. The differential problem (32) can be written in the form of a linear operator $L_{\boldsymbol{s}}(G)$ acting on G

$$\frac{\partial}{\partial t} G = L_{\boldsymbol{s}}(G) \tag{36}$$

where

$$L_{\boldsymbol{s}}(G) = \sum_{i=1}^{M} \left[\lambda_i (s_i - 1) + \left(\sigma_i + \mu_i s_i^2 + \nu_{i+1} s_{i+1} - (\sigma_i + \mu_i + \nu_i) s_i \right) \frac{\partial}{\partial s_i} G \right]$$

As $G = \{K, f\}$, we have

$$\left\{ K, \frac{\partial}{\partial t} f \right\} = \{ L_{\boldsymbol{s}}[K(\boldsymbol{s}, \boldsymbol{a})], f(\boldsymbol{a}, t) \} \tag{37}$$

which is equivalent to

$$\left\{ K, \frac{\partial}{\partial t} f \right\} = \{ K(\boldsymbol{s}, \boldsymbol{a}), M_{\boldsymbol{a}}[f(\boldsymbol{a}, t)] \} \tag{38}$$

where

$$M_{\boldsymbol{a}}[f] = \sum_{i=1}^{M} \mu_i \frac{\partial^2 a_i f}{\partial a_i^2} - \frac{\partial}{\partial a_i} \left[(\lambda_i - a_i(\sigma_i + \nu_i - \mu_i)) f \right] + \nu_{i+1} \frac{\partial a_i f}{\partial a_{i+1}} \tag{39}$$

is the adjoint of $L_{\boldsymbol{s}}(G)$. The governing equation for f is thus a Fokker-Planck equation

$$\frac{\partial}{\partial t} f = M_{\boldsymbol{a}}[f] = - \sum_{i=1}^{M} \frac{\partial}{\partial a_i} [A_i f] + \frac{1}{2} \sum_{i=1}^{M} \frac{\partial^2}{\partial a_i^2} [B_i f] \tag{40}$$

with the drift and diffusion functions

$$A_i \; = \; \lambda_i - \kappa_i a_i - (\nu_i a_i - \nu_{i-1} a_{i-1})$$

$$B_i \; = \; 2 \mu_i a_i$$

where $\kappa_i = \sigma_i - \mu_i$.

4. Analysis of the Langevin representation of b

The Fokker-Planck equation (40) is equivalent to the system of Langevin equations

$$\mathrm{d}a_i = \left(\lambda_i - \kappa a_i - (\nu_i a_i - \nu_{i-1} a_{i-1}) \right) \mathrm{d}t + \sqrt{2 \mu a_i} \mathrm{d}W_i \tag{41}$$

As we stated in the paper, it is very tempting to take the continuum limit of equation (41) by taking $\Delta x \to 0$

$$\frac{\partial b}{\partial t} = \tilde{\lambda} - \kappa b - \frac{\partial}{\partial x} (\bar{u}_p b) + \sqrt{2 \mu b} \xi_b \tag{42}$$

where $\kappa(x,t) = \sigma - \mu$ and λ are a smooth functions, $b(x,t)$ is a continuous function such that $b(x_i) = a_i/\Delta x$ in the limit of $\Delta x \to 0$ and ξ_b is a Gaussian noise term such that $\langle \xi_b(x,t)\xi_b(x',t')\rangle = \delta(x-x')\delta(t-t')$. This equation can be averaged

$$\frac{\partial}{\partial t}\langle b\rangle = \tilde{\lambda} - \kappa\langle b\rangle - \frac{\partial}{\partial x}(\bar{u}_p\langle b\rangle) \tag{43}$$

which is an advection equation with a source term. It admits a homogeneous steady-state solution

$$\langle b\rangle_{ss} = \frac{\tilde{\lambda}}{\kappa}. \tag{44}$$

Far from the boundaries, there is a homogeneous regime, in which the function $b(x,t)$ fluctuates randomly around $\langle b\rangle_{ss}$. What is the variance of these fluctuations? Let us introduce the product $g(x,x',t) = b(x,t)b(x',t)$. Making use of the Itô rule for the differential of dg [*Gardiner*, 1983], we get

$$\begin{aligned} \mathrm{d}g \;=\; & \left[\left(\tilde{\lambda} - \kappa b - \frac{\partial \bar{u}_p b}{\partial x}\right) b(x',t)\right. \\ & + \left(\tilde{\lambda} - \kappa b(x',t) - \frac{\partial \bar{u}_p b'}{\partial x'}\right) b(x,t) \\ & + \left.\mu(b(x',t) + b(x,t))\delta(x-x')\right]\mathrm{d}t \\ & + b(x',t)\sqrt{2\mu b(x,t)}\xi_b(x,t) + b(x,t)\sqrt{2\mu b(x',t)}\xi_b(x',t) \end{aligned} \tag{45}$$

Taking the ensemble average and assuming homogeneous conditions ($\langle b(x,t)\rangle = \langle b(x',t)\rangle$ and $\bar{u}_p$ uniformly constant) state gives

$$\frac{\partial\langle g\rangle}{\partial t} = 2\tilde{\lambda}\langle b\rangle - 2\kappa\langle g\rangle + \bar{u}_p\left(\frac{\partial}{\partial x} + \frac{\partial}{\partial x'}\right)\langle g\rangle + 2\mu\langle b\rangle\delta(x'-x) \tag{46}$$

Under spatially homogeneous conditions, $\langle g\rangle$ depends only on $r = x' - x$. The change of variables $x \to x$ and $x' \to x + r$ leads to

$$\frac{\partial}{\partial x'} = \frac{\partial}{\partial r} \text{ and } \frac{\partial}{\partial x} = \frac{\partial}{\partial x} - \frac{\partial}{\partial r} \tag{47}$$

We end up with the following governing equation for $\langle g \rangle$

$$\frac{\partial \langle g(r,t) \rangle}{\partial t} = 2\tilde{\lambda}\langle b \rangle_{ss} - 2\kappa \langle g \rangle + 2\mu \langle b \rangle_{ss} \delta(r) \tag{48}$$

where the gradient terms have cancelled out.

For steady state conditions ($\partial_t \langle g(r,t) \rangle_{ss} = 0$), we find that the spatial correlation is

$$\langle g \rangle = \frac{\tilde{\lambda} + \mu\delta(r)}{\kappa} \langle b \rangle_{ss} \tag{49}$$

from which we deduce the second order moment

$$\langle g(0) \rangle_{ss} = \frac{\tilde{\lambda} + \mu\delta(0)}{\kappa} \langle b \rangle_{ss} = \tilde{\lambda} \frac{\tilde{\lambda} + \mu\delta(0)}{\kappa^2} \tag{50}$$

and the variance of b under steady state conditions

$$\text{var}_{ss} b = \langle g(0) \rangle_{ss} - \langle b \rangle_{ss}^2 = \frac{\tilde{\lambda}\mu}{\kappa^2} \delta(0) \tag{51}$$

5. Euler scheme for solving the Langevin equation for a_i

The Euler (or Euler-Maruyama) approximation of the Langevin equation

$$da_i(t) = (\lambda_i - a_i(\sigma_i - \mu_i) + \nu_{i-1} a_{i-1} - \nu_i a_i)\, \mathrm{d}t + \sqrt{2\mu_i a_i} \mathrm{d}W_i(t) \tag{52}$$

(with an appropriate initial condition) is the iterative scheme [*Higham*, 2001; *Iacus*, 2008]

$$A_i^{k+1} = A_i^k + \left(\lambda_i - (\kappa_i - \nu_i) A_i^k + \nu_{i-1} A_{i-1}^k\right) \Delta t + \sqrt{2\mu_i A_i} (Z_i^{k+1} - Z_i^k) \tag{53}$$

where $A_i^k = a_i(t_k)$ and $Z_i^k(t) = W_i^k(t_k)$. The discrete times are $t_k = t_{k+1} + \Delta t$.

In practice the random terms $Z_i^{k+1} - Z_i^k$ coming from the difference of the Wiener processes are modeled as $r\sqrt{\Delta t}$ where r is a random number drawn from a uniform distribution ($0 \leq r \leq 1$).The Euler scheme has order 1/2 of strong convergence, i.e. we can find a constant C such that

$$\langle |a(t_k) - A^k| \rangle \leq C\sqrt{\Delta t} \tag{54}$$

6. Iterative calculation of the spatial cross correlations

We have found

$$\operatorname{var} b = \frac{\mu}{\kappa}\langle b\rangle_{ss}\delta(0) = \frac{\mu\tilde{\lambda}}{\kappa^2} \tag{55}$$

which is independent of $\bar{u}_p$! What goes awry with this theory?

Let us return to the discretized equations (41) and let us calculate the second-order moment (making use of the Itô rule)

$$\frac{\mathrm{d}}{\mathrm{d}t}\langle a_i^2\rangle = 2\lambda\langle a_i\rangle - 2(\kappa+\nu)\langle a_i^2\rangle + 2\nu\langle a_i a_{i-1}\rangle + 2\mu\langle a_i\rangle \tag{56}$$

which involves the unknown cross correlation $\langle a_i a_{i-1}\rangle$. Assuming homogeneous steady-state conditions ($\lambda\langle a_i\rangle = \lambda\langle a\rangle$, no time dependence), this equation yields

$$0 = 2\lambda\langle a\rangle_{ss} - 2(\kappa+\nu)\langle a^2\rangle_{ss} + 2\nu\langle a_i a_{i-1}\rangle_{ss} + 2\mu\langle a\rangle_{ss} \tag{57}$$

An evolution equation for the correlation $\langle a_i a_{i-1}\rangle$ is

$$\frac{\mathrm{d}}{\mathrm{d}t}\langle a_i a_{i-1}\rangle = \lambda(\langle a_i\rangle + \langle a_{i-1}\rangle) - 2(\kappa+\nu)\langle a_i a_{i-1}\rangle + \nu\langle a_{i-1}^2\rangle + \nu\langle a_i a_{i-2}\rangle \tag{58}$$

which under steady-state conditions gives

$$0 = 2\lambda\langle a\rangle_{ss} - 2(\kappa+\nu)\langle a_i a_{i-1}\rangle_{ss} + \nu\langle a^2\rangle_{ss} + \nu\langle a_i a_{i-2}\rangle_{ss} \tag{59}$$

which depends $\langle a_i a_{i-2}\rangle_{ss}$. To close the system, let us assume that this term $\nu\langle a_i a_{i-2}\rangle_{ss}$ is zero, then

$$\langle a_i a_{i-1}\rangle_{ss} = \frac{\lambda}{\kappa+\nu}\langle a\rangle_{ss} + \frac{\nu}{2(\kappa+\nu)}\langle a^2\rangle_{ss} \tag{60}$$

and after substitution into equation (57), we get

$$2(\kappa+\nu)\langle a^2\rangle_{ss} = 2(\lambda+\mu)\langle a\rangle_{ss} + 2\nu\left(\frac{\lambda}{\kappa+\nu}\langle a\rangle_{ss} + \frac{\nu}{2(\kappa+\nu)}\langle a^2\rangle_{ss}\right)$$

that is

$$\left(2(\kappa+\nu) - \frac{\nu^2}{\kappa+\nu}\right)\langle a^2\rangle_{ss} = 2\left(\lambda+\mu+\nu\frac{\lambda}{\kappa+\nu}\right)\langle a\rangle_{ss}$$

from which we deduce the following approximation of the variance

$$\operatorname{var}_{ss} a = \frac{2(\lambda+\mu)(\kappa+\nu)+\nu\lambda}{2(\kappa+\nu)^2-\nu^2}\frac{\lambda}{\kappa} - \left(\frac{\lambda}{\kappa}\right)^2 = \frac{\lambda\mu}{(\kappa+\nu)^2}\left(1+\frac{\nu}{\kappa+\nu}+\frac{1}{2}\left(3-\frac{\lambda}{\mu}\right)\frac{\nu^2}{(\kappa+\nu)^2}+O(\nu^2)\right) \tag{61}$$

which depends on ν and gives equation (55) in the limit $\nu \to 0$.

Higher-order approximations can be obtained iteratively by calculating the correlations

$$\langle a_i a_{i-k}\rangle_{ss} = \frac{\lambda}{\kappa+\nu}\langle a\rangle_{ss} + \frac{\nu}{2(\kappa+\nu)}\langle a_i a_{i-k+1}\rangle_{ss} + \frac{\nu}{2(\kappa+\nu)}\langle a_i a_{i-k-1}\rangle_{ss} \tag{62}$$

and closing the system by assuming that at order K, the last correlation term $\langle a_i a_{i-K-1}\rangle_{ss}$ is zero.

Figure 2 shows the variation of $\operatorname{var} a$ with the emigration rate ν. There is clearly a significant effect of ν: the variance of a decreases with increasing ν. The higher the emigration rate, the higher the order of the approximate solution required to get a sufficiently accurate estimate of $\operatorname{var} a$. Note than when ν approaches the CFL limit $(\Delta t)^{-1} = 100$ s^{-1}, the simulation blows up.

7. Iterative calculation of the autocorrelation time

The calculation of the autocorrelation functions obeys the same logic as the spatial cross correlations. We cannot find a closed-form expression, but by using a hierarchy of equations of increasing order, we can deduce an estimate of the autocorrelation function. Let us introduce

$$R_k(\tau|i,t) = \langle a_i(t) a_{i+k}(t+\tau)\rangle - \langle a\rangle^2 \tag{63}$$

We have the hierarchy of equations

$$\dot{R}_0 = -(\kappa+\nu)R_0 + 2\nu R_{-1} \tag{64}$$

$$\dot{R}_{-1} = -(\kappa+\nu)R_{-1} + \nu R_0 + \nu R_{-2} \tag{65}$$

$$\dot{R}_{-2} = -(\kappa+\nu)R_{-2} + \nu R_{-1} \tag{66}$$

$$\vdots$$

To leading order, we have :

$$\rho(t) = \frac{R_0(\tau|i,t)}{R_0(0|i,t)} = \mathrm{e}^{-(\nu+\kappa)t}. \tag{67}$$

8. Stability condition of a central explicit scheme for Langevin equation

We derive the stability condition of the central explicit scheme for the deterministic part of Langevin equation, equation (31) of the manuscript (with $\kappa = \sigma - \mu$),

$$b_j(t+\Delta t) = b_j(t) + \Delta t \left[\tilde{\lambda} - \kappa\, b_j(t) - \frac{\bar{u}_p}{2\Delta x}(b_{j+1}(t) - b_{j-1}(t)) + \frac{D}{\Delta x^2}(b_{j+1}(t) - 2b_j(t) + b_{j-1}(t))\right] \tag{68}$$

that can be rewritten as

$$b_j^{n+1} = b_{j-1}^n \left(r + \frac{\zeta}{2}\right) + b_j^n(1 - 2r - \kappa\Delta t) + b_{j-1}^n \left(r - \frac{\zeta}{2}\right) + \tilde{\lambda}\Delta t \tag{69}$$

with

$$r \equiv D\frac{\Delta t}{\Delta x^2}, \quad \zeta \equiv \bar{u}_p \frac{\Delta t}{\Delta x} \quad b_j^{n+1} = b_j(t+\Delta t), \quad b_j^n = b_j(t) \tag{70}$$

To this end, a von Neumann stability analysis is performed on the base solution $b = \tilde{\lambda}/\kappa$. Introducing an exponential perturbation,

$$b_j^n = \frac{\tilde{\lambda}}{\kappa} + e^{i\,j\,\Delta x\,\xi}, \quad b_j^{n+1} = \frac{\tilde{\lambda}}{\kappa} + g(\xi)\, e^{i\,j\,\Delta x\,\xi}, \quad i = \sqrt{-1} \tag{71}$$

into equation (69), we arrive at the dispersion relation

$$g(\xi)\, e^{i\, j\, \Delta x\, \xi} = e^{i\, j\, \Delta x\, \xi} \left[1 - \kappa \Delta t + r(e^{-i\, \Delta x\, \xi} - 2 + e^{i\, \Delta x\, \xi}) + \frac{\zeta}{2}(e^{-i\, \Delta x\, \xi} - e^{i\, \Delta x\, \xi}) \right] \tag{72}$$

The amplification factor is therefore

$$g(\xi) = 1 - \kappa\, \Delta t + 2\, r\, [-1 + \cos(\xi\, \Delta x)] - i\, \zeta\, \sin(\xi\, \Delta x) \tag{73}$$

The method is stable if $g(\xi)$ lies inside the unitary circle in the complex plane, i.e. if $|g(\xi)| \leq 1$. Taking into account that $-2 \leq \cos(\xi\, \Delta x) - 1 \leq 0$ and $-1 \leq \sin(\xi\, \Delta x) \leq 1$, the method is stable if the following condition holds:

$$\max\{(1 - \kappa\, \Delta t - 4\, r)^2 + \zeta^2, (1 - \kappa\, \Delta t)^2 + \zeta^2\} \leq 1 \tag{74}$$

Substituting the definitions of r and ζ (70) into equation (74) and solving for Δt, we arrive at the stability condition for the time step

$$\Delta t \leq \min \left\{ \frac{(2\, \kappa\, \Delta x^2 + 8\, D)\Delta x^2}{\kappa^2 \Delta x^4 + (\bar{u}_p^2 + 8\, \kappa\, D)\Delta x^2 + 16\, D^2}, \frac{2\, \kappa\, \Delta x^2}{\kappa^2 \Delta x^2 + \bar{u}_p^2} \right\} \tag{75}$$

Therefore, the method is conditionally stable.

We can check that equation (75) correctly predicts well known results in simpler cases:

• The second order centred scheme is unstable for the pure advection equation: setting $\kappa = 0$, $\tilde{\lambda} = 0$, $D = 0$ and $\bar{u}_p \neq 0$ in equation (75), it follows $\Delta t \leq 0$. Therefore, the scheme is unconditionally unstable at all Δt.

• In the pure diffusive case (i.e. $\kappa = 0$, $\tilde{\lambda} = 0$, $\bar{u}_p = 0$, $D \neq 0$) we recover the diffusion stability condition of explicit schemes $\Delta t \leq \Delta x^2 / 2D$.

It is interesting to highlight the stabilizing effect of the parameter κ:

• In the convective-erosion-deposition case (i.e. $D = 0$), the scheme is conditionally stable when $\Delta t \leq 2\kappa \Delta x^2 / (\kappa^2 \Delta x^2 + \bar{u}_p^2)$. In the limit of $\Delta x \to 0$, this condition can be

approximated as $\Delta t \leq 2\kappa\Delta x^2/\bar{u}_p^2 - 2\kappa^3\Delta x^4/\bar{u}_p^4$. The leading order term $\Delta t \leq 2\kappa\Delta x^2/\bar{u}_p^2$ is analogous to the diffusion restriction of the time step with $D = \bar{u}_p^2/4\kappa$.

- Finally, for very thin meshes, $\Delta x \to 0$, equation (75) can be approximated as

$$\frac{\Delta t}{\Delta x^2} \leq \min\left\{\frac{1}{2\,D}\,,\frac{2\kappa}{\bar{u}_p^2}\right\} particle \tag{76}$$

So the stability condition is dominated by the diffusion coefficient D and the deposition rate κ in this limit.

A fully implicit scheme could be formulated to avoid the constraint on the time step. In such a case, Thomas' algorithm could be employed to solve efficiently the tridiagonal system of equations.

9. Variance of diffusive processes

Let us introduce the fluctuating part $b' = b - \langle b\rangle$ in the Langevin equation (102) for b with no advection term ($\bar{u}_p = 0$). The fluctuating part b' satisfies

$$\partial_t b' = d\frac{\partial^2 b'}{\partial x^2} - \kappa b' + \sqrt{2\mu(\langle b\rangle_{ss} + b')}\xi_b \tag{77}$$

This Ito's rule for the change of variable $f = b'^2$ in equation (77) gives

$$\mathrm{d}f = (2b'A + 2\mu b)\,\mathrm{d}t + 2b'\sqrt{2\mu b}\mathrm{d}W + O(\mathrm{d}t) \tag{78}$$

with $A = d\partial_{xx}b - \kappa b'$. If we take the ensemble average, we end up with

$$\frac{\partial}{\partial t}\langle b'^2\rangle = 2\left(d\frac{\partial^2}{\partial x^2}\langle b'^2\rangle - \kappa\langle b'^2\rangle + \mu\langle b\rangle\right) \tag{79}$$

We introduce the variance $\operatorname{var} b = \langle b^2\rangle - \langle b\rangle^2 = \langle b'^2\rangle$ and the spatial covariance $\operatorname{cov} b = \langle b(x,t)b(x+r,t)\rangle - \langle b\rangle^2$. Following the same reasoning that leads us to equation (79) and making use of $b = b' + \langle b\rangle_{ss}$ for the homogeneous region, we find

$$\frac{1}{2}\frac{\partial}{\partial t}\operatorname{cov} b = d\frac{\partial^2}{\partial r^2}\operatorname{cov} b - \kappa\operatorname{cov} b + \mu\langle b\rangle_{ss}\delta(r) \tag{80}$$

This equation is characterized by its steady steady Fourier spectrum

$$-\omega^2 d\mathcal{F} - \kappa\mathcal{F} + \mu\langle b\rangle_{ss} = 0 \tag{81}$$

where

$$\mathcal{F}[f] = \int_{-\infty}^{\infty} \mathrm{e}^{-\imath\omega s} f(s)\mathrm{d}s \tag{82}$$

denotes the Fourier transform. The solution to this algebraic equation is straightforward

$$\mathcal{F}(\omega) = \frac{\mu\langle b\rangle_{ss}}{\kappa + d\omega^2} \tag{83}$$

Taking the inverse Fourier transform leads to

$$\mathrm{cov}_{\,ss} b = \frac{1}{2}\frac{\mu\langle b\rangle_{ss}}{\kappa\ell_c}\mathrm{e}^{-|r|/\ell_c} \text{ with } \ell_c = \sqrt{\frac{d}{\kappa}} \tag{84}$$

from which we deduce the variance by taking $r = 0$

$$\mathrm{var}_{\,ss} b = \frac{1}{2}\frac{\mu\langle b\rangle_{ss}}{\kappa\ell_c} \tag{85}$$

This expression holds for $\Delta x \to 0$ (in practive, when the observation window is very small compared to the correlation length ℓ_c). It may be interesting to calculate an average variance over a control volume of arbitrary length Δx

$$\begin{aligned}\overline{\mathrm{var}_{\,ss} b} &= \frac{1}{\Delta x^2}\frac{1}{2}\frac{\mu\langle b\rangle_{ss}}{\kappa\ell_c}\int_{\Delta x}\int_{\Delta x}\mathrm{e}^{-|x-x'|/\ell_c}\mathrm{d}x\mathrm{d}x', \\ &= \frac{\mu\tilde{\lambda}}{\kappa^2}\frac{\ell_c}{\Delta x^2}\left(\frac{\Delta x}{\ell_c} + \exp\left(-\frac{\Delta x}{\ell_c}\right) - 1\right).\end{aligned} \tag{86}$$

Naturally, in the limit $\Delta x \to 0$, we retrieve the local variance (85).

10. Simulation of advection and diffusion

Here we show numerical simulations of the Langevin equations

$$\begin{aligned}\mathrm{d}a_i(t) &= (\lambda_i - a_i(\sigma_i - \mu_i) + \nu_{i-1}a_{i-1} - \nu_i a_i \\ &+ d_i(a_{i+1} + a_{i-1} - 2a_i))\,\mathrm{d}t + \sqrt{2\mu_i a_i}\mathrm{d}W_i(t)\end{aligned} \tag{87}$$

We solved this system of Langevin equations numerically using an Euler scheme with time step $\mathrm{d}t = 0.01$ s (see section 5) [*Higham*, 2001; *Iacus*, 2008]. The computational domain was split into $M = 100$ cells of length $\Delta x = 1$ m.

We solved an initial boundary value problem with the initial condition $a_i(0) = 1$. We imposed boundary conditions on the left and the right with ghost cells: $a_0 = 0$ and $a_{M+1} = a_M$. We used the same parameters $\lambda = 10\ \mathrm{s}^{-1}$, $\sigma = 5\ \mathrm{s}^{-1}$, $\mu = 4\ \mathrm{s}^{-1}$, $d = 1\ \mathrm{m\ s}^{-2}$. For the advection rate, we took $\nu = 1\ \mathrm{s}^{-1}$, $\nu = 5\ \mathrm{s}^{-1}$, and $\nu = 10\ \mathrm{s}^{-1}$. The dots and gray lines show the numerical simulations. Averages and probabilities were computed over 500 samples once the steady state has been reached (in practice for $t \geq 10$ s).

The mean behavior is obtained by taking the continuum limit

$$\frac{\partial}{\partial t} b(x,t) + \frac{\partial}{\partial x}(\bar{u}_p b) = \frac{\partial^2}{\partial x^2}(Db) + \tilde{\lambda} - (\sigma - \mu) b + \sqrt{2\mu b}\xi_b \tag{88}$$

(with $D = \lim_{\Delta x \to 0} \Delta x^2 d_i$), then the ensemble average

$$\frac{\partial}{\partial t} c(x,t) + \frac{\partial}{\partial x}(\bar{u}_p c) = s(c) + \frac{\partial^2}{\partial x^2}(Dc) \tag{89}$$

subject to $c(x,0) = 1$ and the following boundary condition on the left of the domain $c(0,t) = 0$ and $\partial_x c(L,t) = 0$ with $L = M\Delta x$ (these two conditions are not strictly compatible initially at $x = 0$). The shorthand notation $s(c)$ is the source term $s(c) = \lambda' - (\sigma - \mu)c$.

Under homogeneous steady-state conditions, we have found for the mean value, the covariance, and the variance

$$\langle b \rangle_{ss} = \frac{\tilde{\lambda}}{\sigma - \mu}, \mathrm{cov}_{ss}\, b(r) = \frac{1}{2}\frac{\mu}{\sigma - \mu}\frac{\langle b \rangle_{ss}}{\ell_c} \exp^{-r/\ell_c} \text{ and } \mathrm{var}_{ss}\, b = \frac{1}{2}\frac{\mu}{\sigma - \mu}\frac{\langle b \rangle_{ss}}{\ell_c} \tag{90}$$

with $\ell_c = \sqrt{D/(\sigma - \mu)}$ the correlation length. The autocorrelation function is

$$\rho(t) = \frac{1}{2}\left(\exp\left(-Pe\frac{t}{t_c}\right)\mathrm{Erfc}\left[\left(1-\frac{Pe}{2}\right)\sqrt{\frac{t}{t_c}}\right] + \exp\left(Pe\frac{t}{t_c}\right)\mathrm{Erfc}\left[\left(1+\frac{Pe}{2}\right)\sqrt{\frac{t}{t_c}}\right]\right) \tag{91}$$

with $t_c = (\sigma - \mu)^{-1}$ the correlation time, $\ell_c = \sqrt{D/(\sigma - \mu)}$ the correlation length, and $Pe = \bar{u}_p \ell_c / D$ the Péclet number.

Figure 3 shows the variation of $\langle a_i \rangle_{ss}$ as function of the position i at the final computation time $t = 20$ s. The mean behavior is correctly predicted by the advection diffusion equation (89) (we can make the comparison directly since $\Delta x = 1$ m and $c(x,t) = \varpi_p \langle a_i \rangle_{ss}/\Delta x$ in the limit $\Delta xo0$). There is an excellent agreement between the numerical data (dots) and the solution to the advection diffusion equation (89) for all values of ν tested. Figure 4 shows how $\langle a_k(t) \rangle$ evolves with time at the middle of the computational domain. Again, there is excellent agreement between the advection diffusion equation (89) and the numerical data. As a summary, the mean behavior is well captured by theory. Figure 5 shows particular realizations.

More interestingly, Figure 6 shows the empirical distribution of the numerical data and the theoretical gamma distribution $Ga(\alpha, \beta)$ with three sets of parameters: $\alpha = \lambda/\mu$ and $\beta = \mu/(\sigma - \mu)$ (dashed line) which hold for one-cell systems [*Ancey and Heyman*, 2014], with $\tilde{\alpha} = \langle a \rangle_{ss}^2 / \mathrm{var}_{ss}\, a$ and $\tilde{\beta} = \mathrm{var}_{ss}\, a / \langle a \rangle_{ss}$ (dotted line), where $\mathrm{var}_{ss}\, a$ is deduced from the b variance in equation (85), and $\hat{\alpha} = \langle a \rangle_{ss}^2 / \mathrm{var}_{ss}\, a$ and $\hat{\beta} = \mathrm{var}_{ss}\, a / \langle a \rangle_{ss}$ (solid line), where $\mathrm{var}_{ss}\, a$ is deduced from the b variance in equation (85) but with $\mathcal{D} = D + D_*$ instead of D. The one-cell solution is unable to describe the empirical distribution. For $\nu = 1$ s^{-1}, the difference between the two diffusion solutions is so tiny that it is not visible. For $\nu = 5$ s^{-1} and $\nu = 10$ s^{-1}, the differences are marked. The distribution

$Ga(\hat{\alpha}, \hat{\beta})$ closely matches the numerical data, confirming that particle advection produces diffusion-like effects.

Figure 7 shows the autocorrelation functions. For $\nu = 1$ s^{-1}, the theoretical function (91) properly describes the empirical autocorrelation function. For $\nu = 5$ s^{-1} and $\nu = 10$ s^{-1}, the correction $D \to \mathcal{D} = D + D_*$ provides the correct trend.

11. Analytical solution to the pure advection solution

Here we provide the analytical solution to the pure advection equation [referred to as equation (20) in the paper]

$$\frac{\partial}{\partial t} c(x,t) + \frac{\partial}{\partial x}(\bar{u}_p c) = s(c) \tag{92}$$

where the source term is $s(c) = \lambda' - (\sigma - \mu)c = \lambda' - \kappa c$ and the advection velocity $\bar{u}_p$ is assumed constant. We consider the following boundary initial value problem

$$c(0,t) = 0 \text{ for } t \geq 0 \text{ and } c(x,0) = f(x) \text{ for } x \geq 0 \tag{93}$$

where f is a positive function satisfying $f(0) = 0$ for the consistency of the initial and boundary conditions. We use the method of characteristics [*Zauderer*, 1983] and cast equation (92) in the following form

$$\frac{\mathrm{d}c}{\mathrm{d}\zeta} = \lambda' - \kappa c \text{ along the characteristic curve } \frac{\mathrm{d}x}{\mathrm{d}\zeta} = \bar{u}_p \tag{94}$$

where we have introduced the dummy variable ζ. To solve this boundary initial value problem, we take advantage from the fact that the characteristic curves are all parallel (with slope $\bar{u}_p^{-1}$). It is us possible to break down the original problem into an initial value problem (domain 1) and a boundary value problem (domain 2), as shown by Figure 8.

We first solve the system of characteristic equations for domain 1 (see Figure 8)

$$\frac{\partial t}{\partial \zeta} = 1, \frac{\partial x}{\partial \zeta} = \bar{u}_p \text{ and } \frac{\partial c}{\partial \zeta} = s(c) \tag{95}$$

with the initial data written parametrically as

$$x(\zeta = 0) = x_1, t(\zeta = 0) = 0 \text{ and } c(\zeta = 0) = f(x_1) \tag{96}$$

The integration is straightforward

$$c_1(x,t) = \frac{\mathrm{e}^{-\kappa t}}{\kappa} \left(\kappa f(x - \bar{u}_p t) + \lambda'(\mathrm{e}^{\kappa t} - 1) \right). \tag{97}$$

We now solve the system of characteristic equations for domain 2 (see Figure 8)

$$\frac{\partial t}{\partial \zeta} = 1, \frac{\partial x}{\partial \zeta} = \bar{u}_p \text{ and } \frac{\partial c}{\partial \zeta} = s(c) \tag{98}$$

The initial data for the boundary value problem can be written parametrically as

$$x(\zeta = 0) = 0, t(\zeta = 0) = t_1 \text{ and } c(\zeta = 0) = 0 \tag{99}$$

The solution is readily found

$$c_2(x,t) = \frac{\lambda'}{\kappa} \left(1 - \exp\left(-\frac{\kappa x}{\bar{u}_p} \right) \right) \tag{100}$$

The full solution to the boundary initial value problem is thus

$$c(x,t) = \begin{cases} c_1(x,t) & \text{for } x \geq \bar{u}_p t, \\ c_2(x,t) & \text{for } x < \bar{u}_p t. \end{cases} \tag{101}$$

Figure 9 shows the exact solution to the boundary initial value problem considered in Figure 2 in the body of the paper.

12. Expressing $\langle a \rangle$ as a convolution sum

Let us take the ensemble average of the Langevin equation (41)

$$\frac{\mathrm{d}}{\mathrm{d}t}\langle a_i \rangle = \lambda_i - \kappa_i \langle a_i \rangle - (\nu_i \langle a_i \rangle - \nu_{i-1} \langle a_{i-1} \rangle) \text{ for } 1 \leq i \leq M \tag{102}$$

Under steady state (not necessarily homogeneous) conditions, we can recast the latter system of equations in matrix form

$$\boldsymbol{A} \cdot \langle \boldsymbol{a} \rangle = \boldsymbol{\Lambda}, \tag{103}$$

where $\boldsymbol{\Lambda}$ is the column vector $(\lambda_i)_{1 \leq i \leq M}$ and $\boldsymbol{A}$ is a $M \times M$ lower bidiagonal matrix, whose main diagonal elements are $\kappa_i + \nu_i$ $(1 \leq i \leq M)$ and the lower diagonal entries are $-\nu_{i-1}$ $(1 \leq i \leq M-1)$ (all other entries are zero). The inverse of a lower bidiagonal matrix is a lower triangular matrix $\boldsymbol{L}$, whose entries can be calculated exactly [e.g., see section 4.3 of *Vandebril et al.*, 2008]. We introduce the $M \times M$ diagonal matrix $\boldsymbol{K}$, whose diagonal terms are $K_i = \kappa_i + \nu_i$ and the $M \times M$ elementary matrix $\boldsymbol{Q}_i = \boldsymbol{I} - q_i \boldsymbol{e}_{i+1} \boldsymbol{e}_i$, where $\boldsymbol{e}_i$ denotes the vector of length M in which all but one entry is zero: $e_i = 1$, $e_k = 0$ for $k \neq i$, $\boldsymbol{I}$ is the identity matrix, and $q_i = -\nu_i / (\kappa_{i+1} + \nu_{i+1})$. The inverse of $\boldsymbol{L}$ is the matrix product

$$\boldsymbol{L} = \boldsymbol{A}^{-1} = \boldsymbol{K}^{-1} \cdot \boldsymbol{Q}_{M-1} \cdots \boldsymbol{Q}_2 \cdot \boldsymbol{Q}_1 \tag{104}$$

This is a $M \times M$ lower triangular matrix whose entries are

$$L_{ij} = \begin{cases} 0 & \text{if } j > i \\ (\kappa_{i+1} + \nu_{i+1})^{-1} & \text{if } j = i \\ \dfrac{1}{\kappa_{i+1} + \nu_{i+1}} \displaystyle\prod_{k=1}^{i-j} \frac{\nu_{M-k}}{\kappa_{M-k} + \nu_{M-k}} & \text{if } j < i \end{cases} \tag{105}$$

The steady state solution can thus be expressed as a convolution sum

$$\langle \boldsymbol{a} \rangle = \boldsymbol{L} \cdot \boldsymbol{\Lambda} \tag{106}$$

or said differently, this means that the Poisson rate at cell i depends on all upstream positions

$$\langle a_i \rangle = \sum_{k=1}^{i} L_{ij} \lambda_j \text{ for } 1 \leq i \leq M \tag{107}$$

Let us now assume that the system is also homogeneous so that $\lambda_i = \lambda$, $\kappa_i = \kappa$, and $\nu_i = \nu$ for $1 \leq i \leq M$. After simple algebraic manipulations, we find that

$$\langle a_i \rangle = \lambda \sum_{k=1}^{i} \frac{\nu^{k-1}}{(\kappa + \nu)^k} \tag{108}$$

Let us make use of the change of variable $\zeta = \nu/(\kappa + \nu)$ and recast equation (108) in the form of geometric series

$$\langle a_i \rangle = \frac{\lambda}{\nu} \zeta \sum_{k=0}^{i-1} \zeta^k = \frac{\lambda}{\nu} \frac{1 - \zeta^i}{1 - \zeta} \tag{109}$$

As $\zeta < 1$, we find that in the limit $i \to \infty$,

$$\langle a_i \rangle \approx \frac{\lambda}{\nu} \frac{\zeta}{1 - \zeta} = \frac{\lambda}{\kappa} \tag{110}$$

which is the steady state solution under homogeneous conditions, $\langle a \rangle_{ss} = \lambda/\kappa$ given by equation (16) in the paper. In general, the series converges quickly to the steady state value $\langle a \rangle_{ss}$. Figure 10 shows an example of calculation: for cell $i = 1$, there is no particle entering this cell and so the steady state value is $\langle a_1 \rangle = \lambda/(\kappa + \nu)$. For $i > 6$, the homogeneous steady-state value $\langle a \rangle_{ss} = \lambda/\kappa = 10$ is reached to within 1%.

References

Allen, E. J. (2007), *Modeling with Itô Stochastic Differential Equations*, Springer, New York.

Ancey, C., and J. Heyman (2014), A microstructural approach to bed load transport: mean behaviour and fluctuations of particle transport rates, *J. Fluid Mech.*, *744*, 129–168.

Gardiner, C. W. (1983), *Handbook of Stochastic Methods*, Springer Verlag, Berlin.

Gillespie, D. T. (2001), Approximate accelerated stochastic simulation of chemically reacting systems, *J. Chem. Phys.*, *115*, 1716–1733.

Higham, D. J. (2001), An algorithmic introduction to numerical simulation of stochastic differential equations, *SIAM Rev.*, *43*, 525–546.

Iacus, S. M. (2008), *Simulation and Inference for Stochastic Differential Equations*, Springer, New York.

Vandebril, R., M. Van Barel, and N. Mastronardi (2008), *Matrix Computations and Semiseparable Matrices, Volume 1: Linear Systems*, The Johns Hopkins University Press, Baltimore.

Zauderer, E. (1983), *Partial Differential Equations of Applied Mathematics*, Pure and Applied Mathematics, John Wiley & Sons, New York.

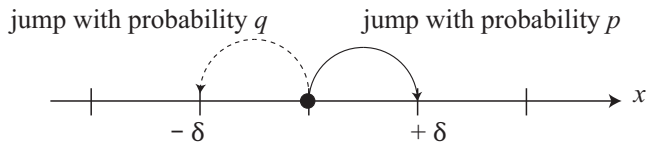

Figure 1. Random walk: the particle can jump to the right with probability p or to the left with probability q at each time step. It can stay at the same place with probability r.

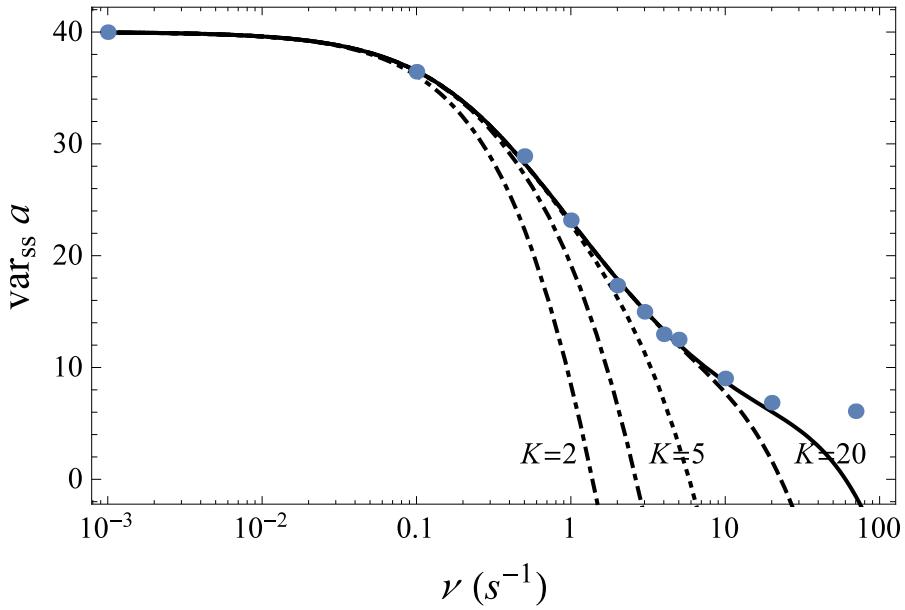

Figure 2. Variation of the variance $\mathrm{var}\, a$ as a function of the advection rate ν. Approximate solutions to order $K = 1$ (black solid line) given by equation (61), $K = 3$ (dot-dashed line), $K = 5$ (dotted line), $K = 10$ (dashed line), and $K = 20$ (blue solid line). Simulations done for $\Delta x = 1$, with $M = 100$ cells, time increment $\mathrm{d}t = 0.01$ s, parameters $\lambda = 10\ \mathrm{s}^{-1}$, $\mu = 4\ \mathrm{s}^{-1}$, $\sigma = 5\ \mathrm{s}^{-1}$ (thus $\kappa = 1\ \mathrm{s}^{-1}$). Initial state: $a_i = 1$ for $1 \leq i \leq M$. Boundary condition $a_0 = 0$. The samples were simulated 200 times.

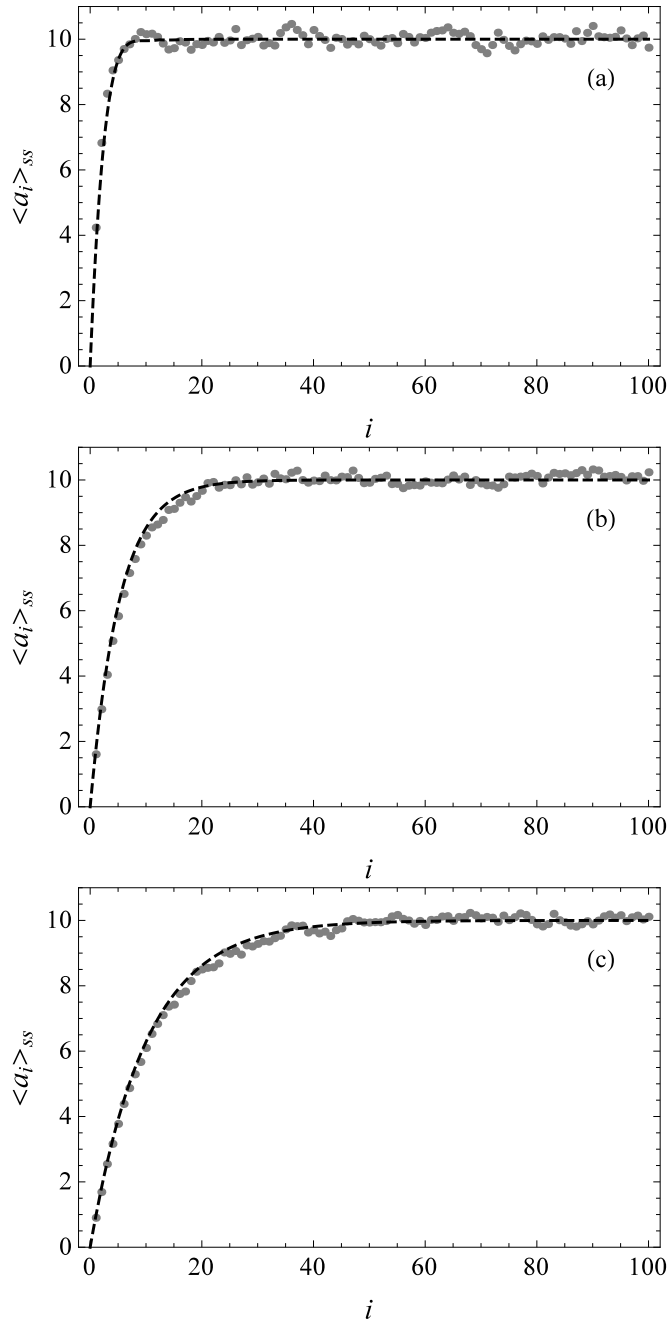

Figure 3. Example of simulation of the Langevin equations (87): variation of $\langle a_i \rangle_{ss}$ as function of the position i ($1 \leq i \leq M$) at time $t = 20$ s. The dashed line shows the pure advection behavior obtained by solving the advection diffusion equation (89) numerically. (a) $\nu = 1$ s^{-1}, (b) $\nu = 5$ s^{-1}, and (c) $\nu = 10$ s^{-1}

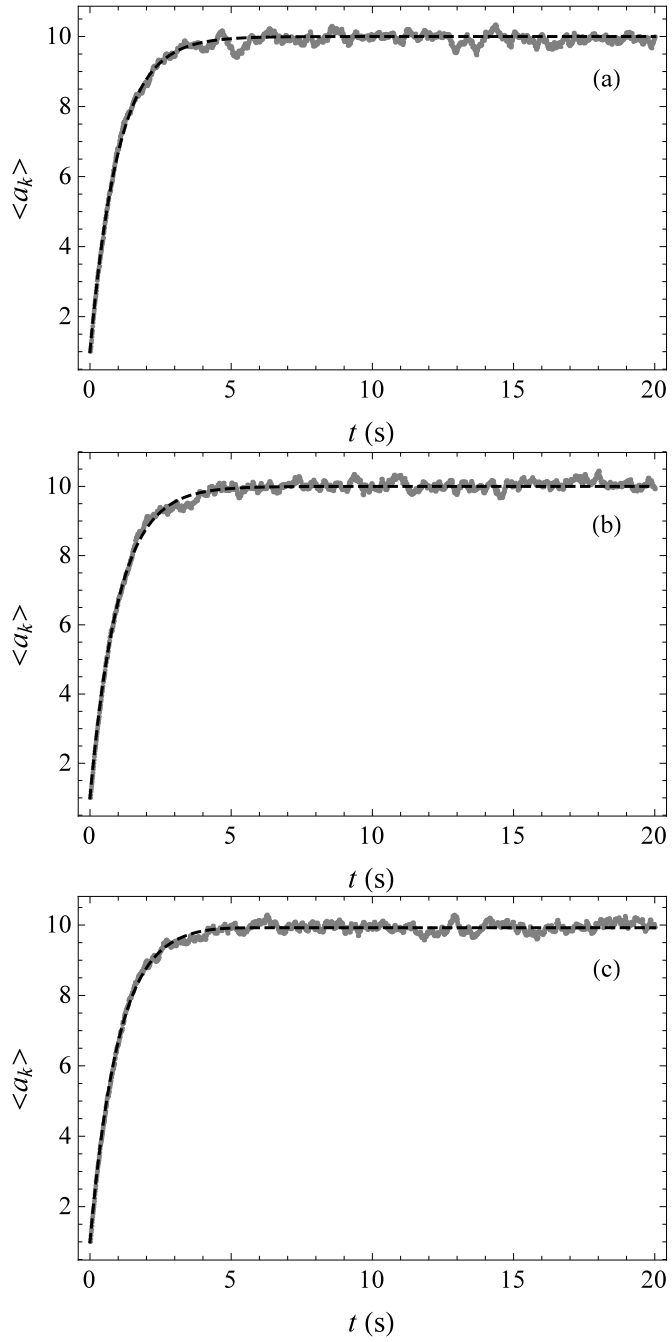

Figure 4. Example of simulation of the Langevin equations (87): time variation of $\langle a_k(t) \rangle$ for $k = 50$ (middle of the computational domain). The dashed line shows the pure advection behavior obtained by solving the advection diffusion equation (89) numerically. (a) $\nu = 1$ s^{-1}, (b) $\nu = 5$ s^{-1}, and (c) $\nu = 10$ s^{-1}

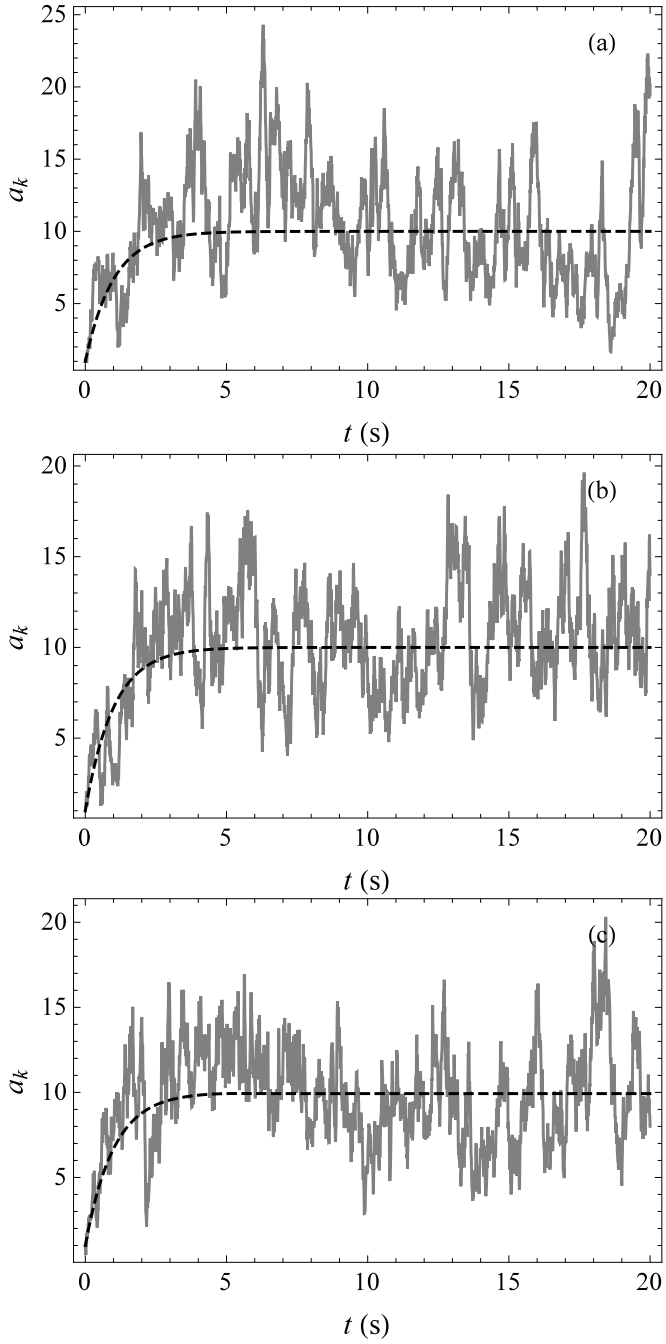

Figure 5. Example of simulation of the Langevin equations (87): particular realization of the process $a_k(t)$ for $k = 50$. The dashed line shows the pure advection behavior obtained by solving the advection equation (89) numerically. (a) $\nu = 1$ s^{-1}, (b) $\nu = 5$ s^{-1}, and (c) $\nu = 10$ s^{-1}

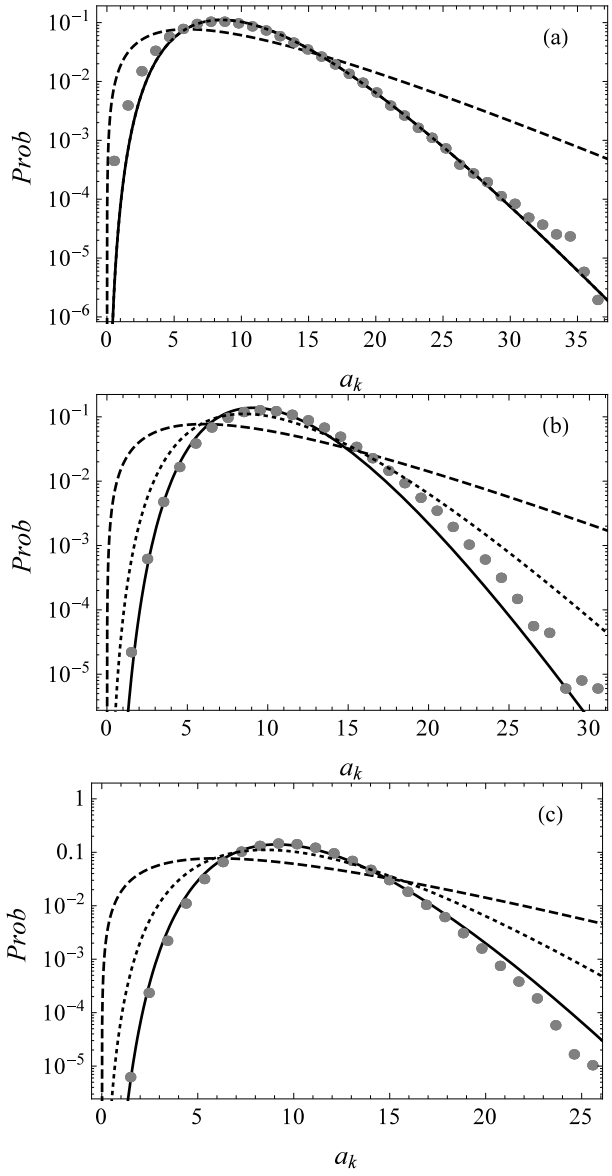

Figure 6. Example of simulation of the Langevin equations (87): probability distribution function of a_k for $k = 50$. The dashed line is the gamma distribution $Ga(\alpha, \beta)$, with $\alpha = \lambda/\mu$ and $\beta = \mu/(\sigma - \mu)$, the parameters found for the one-cell system [*Ancey and Heyman*, 2014]. The dotted line shows the gamma distribution $Ga(\alpha, \beta)$ with $\tilde{\alpha} = \langle a \rangle_{ss}^2 / \mathrm{var}_{ss}\, a$ and $\tilde{\beta} = \mathrm{var}_{ss}\, a / \langle a \rangle_{ss}$, where $\mathrm{var}_{ss}\, a$ is deduced from the b variance in equation (85) by taking $\mathrm{var}_{ss}\, a = \Delta x^2 \overline{\mathrm{var}\, b}$. The solid line is the gamma distribution $Ga(\hat{\alpha}, \hat{\beta})$, with the diffusivity corrected as $\mathcal{D} = D + D_*$ with $D_* = \nu \Delta x^2/2$. (a) $\nu = 1$ s^{-1}, (b) $\nu = 5$ s^{-1}, and (c) $\nu = 10$ s^{-1}.

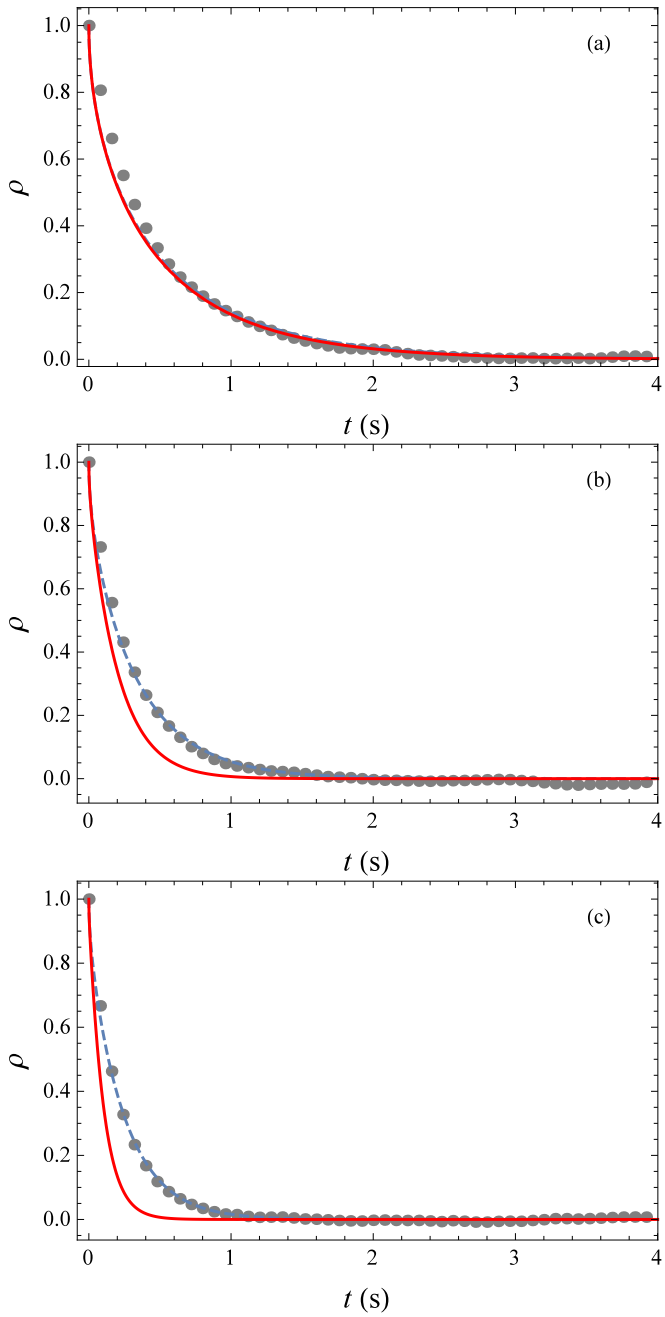

Figure 7. Autocorrelation functions: the dots shows the empirical autocorrelation function for cell $k = 50$. The red solid line shows the theoretical autocorrelation function (91) and the blue dashed line represents the same function (91), but with D replaced by $\mathcal{D} = D + D_*$. (a) $\nu = 1$ s^{-1}, (b) $\nu = 5$ s^{-1}, and (c) $\nu = 10$ s^{-1}. The empirical autocorrelation function has been obtained by averaging 500 particular autocorrelation functions.

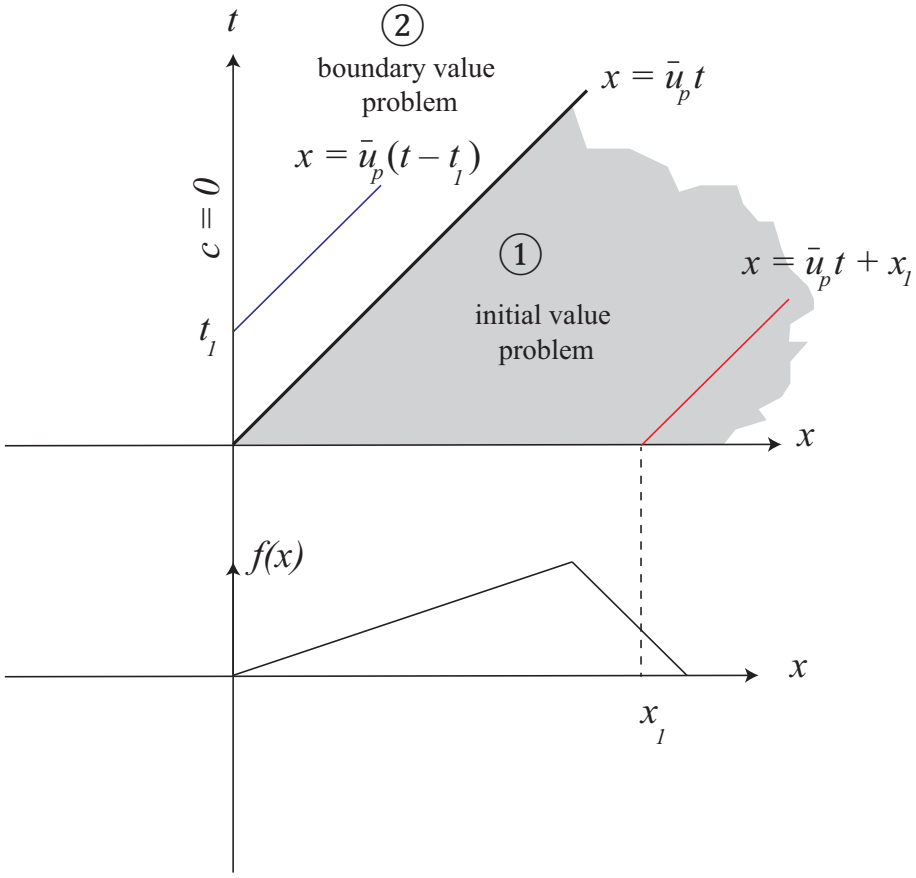

Figure 8. Characteristic diagram. The upper plot shows the family of characteristic curves $x(s)$ in the $x-t$ plane. The characteristic curve $x = \bar{u}_p t$ issuing from the origin point divides the first quadrant into two domains: domain 1 corresponds to the initial value problem, while domain 2 pertains to the boundary value problem. All the characteristic curves are parallel. The lower plot shows the initial condition $c(x, 0) = f(x)$.

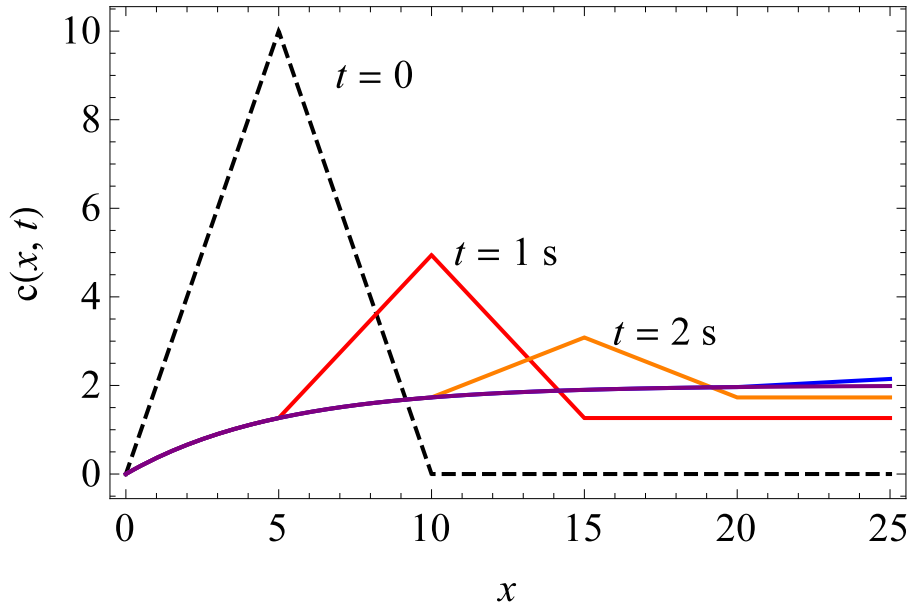

Figure 9. Solutions to the boundary initial value problem (92)–(93). The solid lines show the exact solution (101) calculated at times $t = 1$ s, 2 s, 4 s and 8 s. The dashed line shows the initial condition $f(x) = x$ for $0 \leq x \leq 5$ m, $f(x) = 10 - x$ for $5 \leq x \leq 10$ m, and $f(x) = 0$ elsewhere. Calculation achieved with $\lambda = 2\ \mathrm{s}^{-1}$, $\kappa = 1\ \mathrm{s}^{-1}$, $\bar{u}_p = 5\ \mathrm{m\,s}^{-1}$.

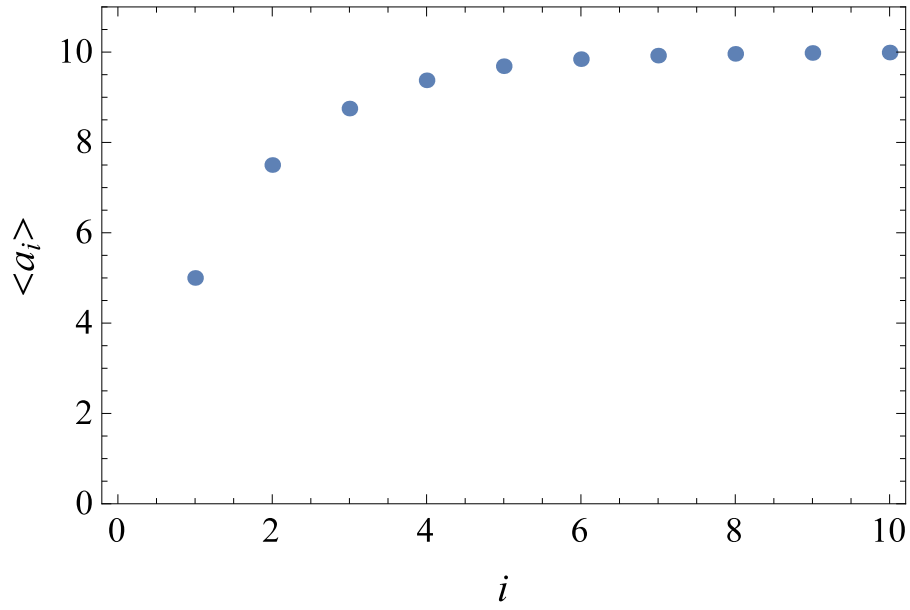

Figure 10. Variation in the steady state $\langle a_i \rangle$ with i. Calculation done with $\lambda = 10$ s^{-1}, $\sigma = 5$ s^{-1}, $\mu = 4$ s^{-1}, $\nu = 5$ s^{-1} ($\kappa = 1$ s^{-2}).